

# Investigation on laser selective photoionisation of the $^{177\text{m}}\text{Lu}$ isomer

A.B. D'yachkov, A.A. Gorkunov, A.V. Labozin, K.A. Makoveeva,  
S.M. Mironov, V.A. Firsov, G.O. Tsvetkov, V.Ya. Panchenko

**Abstract.** The selectivity of laser photoionisation of  $^{177\text{m}}\text{Lu}$  nuclear isomer with respect to natural isotopes has been studied for the first time using a three-stage lutetium photoionisation scheme  $5d6s^2D_{3/2} - 5d6s6p^4F_{5/2}^o - 5d6s7s^4D_{3/2} - (53375 \text{ cm}^{-1})_{1/2}^o$ .

**Keywords:** laser selective photoionisation, lutetium-177, nuclear medicine.

## 1. Introduction

Currently, lutetium-177 radionuclide ( $^{177}\text{Lu}$ , half-life 6.7 days) is increasingly used in medical practice and biological research due to the low energy of beta radiation (490 keV) and soft concomitant gamma radiation (208.37 and 112.98 eV) that allows the accumulation of drugs to be controlled *in vivo* [1]. Lutetium in nature is represented by two isotopes:  $^{175}\text{Lu}$  (content 97.4%) and  $^{176}\text{Lu}$  (content 2.6%). The  $^{177}\text{Lu}$  isotope is artificial, and two methods are mainly used for its production, based on neutron irradiation in nuclear reactors of isotopically enriched  $^{176}\text{Lu}$  or  $^{176}\text{Yb}$  isotopes. Irradiation of  $^{176}\text{Lu}$ , along with  $^{177}\text{Lu}$ , forms a long-lived  $^{177\text{m}}\text{Lu}$  isomer (half-life 160.4 days) [2], the presence of which in the preparation presents certain difficulties for medical institutions in terms of waste storage and disposal. New technological possibilities for the isolation of the  $^{177\text{m}}\text{Lu}$  isomer from an irradiated natural mixture of lutetium isotopes are opening up with the use of selective laser photoionisation [3–5].

In work [3], the following scheme of lutetium photoionisation was proposed and investigated:  $5d6s^2D_{3/2} - 5d6s6p^4F_{5/2}^o - 5d6s7s^4D_{3/2} - (53375 \text{ cm}^{-1})_{1/2}^o$  [(53375  $\text{cm}^{-1}$ ) $_{1/2}^o$  is unidentified autoionisation level]. Its efficiency was investigated in work [4], and the selectivity of the  $^{177}\text{Lu}$  isotope photoionisation was studied in work [5]. The photoionisation scheme levels have a developed hyperfine structure, which, together with the selection rules, gives more than 40 different combinations of sublevels, i.e. channels that can be used for photoionisation. The difference in the transition frequencies of different channels of the same isotope, as a rule, significantly exceeds the width of the laser radiation spectrum, and thus, with certain laser tuning, it is possible to perform photoionisation by

a single channel. In work [6], the isotopic shifts and hyperfine structure constants of the  $^{177\text{m}}\text{Lu}$  isomer were determined, and also photoionisation channels were identified to allow selective isomer isolation. An important step in the development of the analytical method of laser resonance ionisation mass spectrometry [7] is the experimental study on the photoionisation selectivity of the  $^{177\text{m}}\text{Lu}$  isomer with respect to the  $^{175}\text{Lu}$  and  $^{176}\text{Lu}$  natural isotopes, as well as with respect to the  $^{177}\text{Lu}$  isotope. This work is dedicated to the study on the photoionisation selectivity of the  $^{177\text{m}}\text{Lu}$  isomer with respect to natural isotopes.

## 2. Experiment

The studies were performed on a setup designed for experiments on laser photoionisation spectroscopy in narrow collimated atomic beams with the possibility of determining the isotopic composition of photoions. The setup consisted of a vacuum chamber with an evacuation system, an evaporator, and an MC-7302 quadrupole mass spectrometer. The atomic beam formed by the evaporator entered the ion source of the mass spectrometer. For resonant excitation and ionisation of atoms, we used radiation from three pulsed single-mode dye lasers [spectral line width of 100–120 MHz (FWHM), pulse duration of 20–25 ns, repetition rate of 10 kHz] pumped by radiation from copper vapour lasers. The laser beams crossed the atomic beam directly in the ion source ionisation chamber. The directions of the atomic and laser beams and the ion-optical axis of the mass spectrometer were mutually orthogonal. Ions in the mass spectrometer were recorded by a secondary electron multiplier. To control the lasing wavelength of dye lasers, LM-007 precision wavelength meters (Laser 2000 GmbH, Germany) were used, providing an absolute wavelength measurement accuracy of 0.0005 Å. The setup control and data recording were performed online. The software, implemented in the LabView environment (National Instruments Copr., USA), performed the necessary actions, which included, among other things, receiving signals from the secondary electron multiplier and data from the wavelength meters, as well as varying the control voltage using the interface unit to stabilise each dye laser by the wavelength or, if necessary, to scan the wavelength. The technical parameters and experimental setup features are described in detail in works [8, 9].

The  $^{177\text{m}}\text{Lu}$  isomer was obtained by irradiating 0.6 g of natural metallic lutetium in the IR-8 reactor by a neutron flux of  $1.4 \times 10^{13} \text{ cm}^{-2} \text{ s}^{-1}$  for 49 days. The isomer concentration was determined by gamma spectrometry using the 319.02- and 413.62-keV lines (their relative intensities were 10.5% and 17.5%, respectively). At the time of the experiments (10

A.B. D'yachkov, A.A. Gorkunov, A.V. Labozin, K.A. Makoveeva,  
S.M. Mironov, V.A. Firsov, G.O. Tsvetkov, V.Ya. Panchenko National  
Research Centre 'Kurchatov Institute', pl. Akad. Kurchatova 1,  
123182 Moscow, Russia, e-mail: Tsvetkov\_GO@nrcki.ru

Received 9 December 2020  
Kvantovaya Elektronika 51 (4) 317–319 (2021)  
Translated by M.A. Monastyrsky

months after irradiation), the  $^{177\text{m}}\text{Lu}$  content in the sample was  $(1.2 \pm 0.1) \times 10^{-6}$ . The activity ratio of the  $^{177}\text{Lu}$  isotope and the  $^{177\text{m}}\text{Lu}$  isomer, determined from the intensities of the 112.98- and 208.37-keV lines (minus the  $^{177\text{m}}\text{Lu}$  radiation intensity on these lines), was  $0.2 \pm 0.03$ , which corresponds to the  $^{177}\text{Lu}$  isotope content of  $(1 \pm 0.2) \times 10^{-8}$ .

Photoionisation of the  $^{177\text{m}}\text{Lu}$  isotope was performed according to the three-stage scheme  $5d6s^2D_{3/2} - 5d6s6p^4F_{5/2}^0 - 5d6s7s^4D_{3/2} - (53375 \text{ cm}^{-1})_{1/2}^0$ . We used four channels with the participation of various components of the hyperfine structure (HFS), which had the total moments  $F$  with the largest shifts in the transition frequencies from the frequencies of the nearest transitions of the ionisation channels of natural lutetium isotopes [6] (Table 1). The pulses of the second and third stage lasers were delayed relative to the first stage pulse by the pulse duration ( $\sim 20$  ns). The experiments were performed with the same parameters of the laser pulses: the average power densities of laser radiation in the stages were 6, 4, and 2500  $\text{mW cm}^{-2}$ , respectively. The  $^{177\text{m}}\text{Lu}$  photo-currents for all ionisation channels were comparable and corresponded to the region of the photocurrent transition to the saturation mode (in terms of radiation intensity).

The mass spectra of photoions in the  $^{177\text{m}}\text{Lu}$  ionisation by 12-13-13-12 and 13-13-13-12 channels (the numbers indicate the values of the total moments  $F$  of the HFS sublevels used) are shown in Fig. 1. With a mass of 177, the photoions of the  $^{177\text{m}}\text{Lu}$  isomer, on the absorption line of which the lasers are tuned, and also the  $^{177}\text{Lu}$  photoions, contribute to the mass spectrometer signal. However, due to the fact that the initial  $^{177}\text{Lu}$  content is two orders of magnitude less than the  $^{177\text{m}}\text{Lu}$  isomer content, the contribution of the  $^{177}\text{Lu}$  isotope signal can be neglected.

The experimental results are summarised in Table 1, where, for each channel, the excitation channels of natural isotopes having the closest values of the transition frequencies are indicated, along with the frequency distances to the  $^{177\text{m}}\text{Lu}$  transition frequencies for all ionisation stages. This Table also

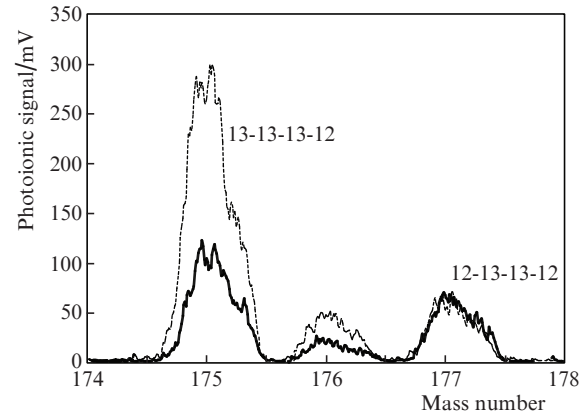


**Figure 1.** Mass spectra of photoions in the  $^{177\text{m}}\text{Lu}$  ionisation by the 12-13-13-12 and 13-13-13-12 channels.

presents selectivity as the ratio of the probabilities of laser photoionisation of the isomer and the corresponding isotope. The last column shows the total selectivity  $S$  of the isomer photoionisation with respect to natural isotopes, calculated by the formula

$$S = \frac{C_p(1 - C_f)}{C_f(-C_p)},$$

where  $C_f$  is the original content of the target isotope  $^{177\text{m}}\text{Lu}$ ; and  $C_p$  is the concentration of the  $^{177\text{m}}\text{Lu}$  photoions.

The maximum selectivity  $S = 5.5 \times 10^5$  ( $C_p = 0.4$ ) was obtained in ionisation via the 12-13-13-12 channel. The decrease in selectivity when using 13-13-13-12 and 10-10-10-11 channels is probably associated with smaller isotopic shifts in the  $^{175}\text{Lu}$  levels at the first stage. On the other hand, the ionisation selectivity by the 12-12-13-12 channel with the largest isotopic shift of the radiation frequency at the first stage

**Table 1.** Characteristics of the  $^{177\text{m}}\text{Lu}$  selective photoionisation channels.

$F_{177\text{m}}$	$\lambda/\text{\AA}$ [9]	$F_{175}$	$\nu_{175} - \nu_{177\text{m}}/\text{MHz}$ [6]	$F_{176}$	$\nu_{176} - \nu_{177\text{m}}/\text{MHz}$ [6]	$S_{175}/10^5$	$S_{176}/10^5$	$S/10^5$
12-	5404.0261	4-	-996	17/2-	-1110			
13-	5350.5966	5-	+1267	17/2-	+995	7.5(5)	0.62(5)	5.5(5)
13-	6180.1151	5-	+235	17/2-	-927			
12		4		15/2				
13-	5404.0474	5-	-852	17/2-	+1078			
13-	5350.5966	5-	+1267	17/2-	+995	2.0 (2)	0.32(2)	1.8(2)
13-	6180.1151	5-	+235	17/2-	-927			
12		4		15/2				
12-	5404.0677	5-/4-	+1232/+3276	13/2-	+298			
12-	5350.5558	5-	-3005	15/2-	+2858	2.4(2)	0.48(5)	2.2(2)
13-	6180.1151	5-	+235	17/2-	-927			
12		4		15/2				
10-	5404.1342	3-	-832	15/2-	+1274			
10-	5350.6117	2-	+880	13/2-	+1225	1.2(1)	0.17(2)	1.0(1)
10-	6180.0395	2-	+545	13/2-	-3640			
11		3		13/2				

Note:  $F_{177\text{m}}$ ,  $F_{175}$ , and  $F_{176}$  – are the  $F$  values of the HFS sublevels in the  $^{177\text{m}}\text{Lu}$ ,  $^{175}\text{Lu}$ , and  $^{176}\text{Lu}$  ionisation channels;  $\lambda$  is the radiation wavelength of the ionisation stages;  $\nu_{175} - \nu_{177\text{m}}$  is the shift of the radiation frequency  $\nu_{175}$  of the  $^{175}\text{Lu}$  ionisation stage from the radiation frequency  $\nu_{177}$  of the  $^{177\text{m}}\text{Lu}$  ionisation stage; and  $\nu_{176} - \nu_{177\text{m}}$  is the shift of the radiation frequency  $\nu_{176}$  of the  $^{176}\text{Lu}$  ionisation stage from the radiation frequency  $\nu_{177\text{m}}$  of the  $^{177\text{m}}\text{Lu}$  ionisation stage.

(1.23 GHz) was also relatively low. The reason for this may be as follows. Despite the fact that the dye laser mainly implements single-mode lasing on a single longitudinal mode, there is a possibility of generating side (neighbouring) low-intensity modes. The frequency distance between the longitudinal modes is determined by the cavity length (in our case, 110–140 mm) and lies in the range of 1100–1360 MHz. The approach of the side mode to the transition frequency of the non-target isotope (the first transition 12-12) affects the process selectivity. This can be especially noticeable under conditions of low isomer content. Judging by the spectral profile of the lasing line, a decrease in the relative concentration of photoions of the target isotope may become noticeable even when the side modes contain  $10^{-4}$  of the total laser power.

When the laser pulses were synchronised, a sharp (by two orders of magnitude) decrease in the selectivity of photoionisation was observed. Due to the low isomer content, the selectivity in this case could only be measured by using the 12-13-13-12 channel and was  $S = 6 \times 10^3$ . When using other channels, the selectivity was even lower and could not be determined due to the insufficient dynamic range of the mass spectrometer. Additional photoionisation of non-target isotopes occurred due to the appearance of nonresonant two-photon absorption from the ground state of Lu atoms [10]. The probability of such transitions is largely determined by the difference between the sum of the energies of the radiation quanta of the first and second stages from the energy of the second excited state of the non-target isotope ( $^{175}\text{Lu}$ ), which for all channels did not exceed  $\sim 400$  MHz.

The upper limit of the photoionisation efficiency can be determined from the behaviour of the experimental dependences of the photoion signal on the laser intensity. Low intensities correspond to a linear increase in the photoion signal, which, with increasing intensity, passes over into the saturation regime. The reason for saturation is the emptying of atoms from the lower state. When the signal is saturated, the photoionisation efficiency is proportional to the original population of the atomic level. At an evaporation temperature of  $1700^\circ\text{C}$ , 0.77 of all  $^{177\text{m}}\text{Lu}$  atoms are located at the original  $5d6s^2D_{3/2}$  level. The level consists of four sublevels with quantum numbers  $F = 10, 11, 12, 13$ , which are populated in proportion to their statistical weights  $2F + 1$ . Thus, for the sublevel with  $F = 12$ , the population was 26% and, therefore,  $0.77 \times 26\% \approx 20\%$  of isomer atoms could be converted into photoions.

If the radiation pulses of the second and third stages are delayed relative to the first-stage pulse, the photoionisation efficiency decreases. It only involves the atoms that remain in the first excited state (lifetime 472 ns) after the first-stage pulse termination. After the first transition has been saturated, the fraction of such atoms is determined as the ratio of the statistical weights of the upper and lower sublevels. For the 12-13 transition, this ratio is 0.52, and the upper limit of the ionisation efficiency is reduced to  $\sim 10\%$ . The photoionisation efficiency according to this scheme was experimentally investigated in work [4].

The maximum increase in the photoionic signal of the isomer in the case when the radiation pulses of three stages coincide in time and the average intensity consistently increases in stages to  $96, 30 \text{ mW cm}^{-2}$ , and  $4 \text{ W cm}^{-2}$  is 95%, which is in good agreement with the estimate of the decrease in the photoionisation efficiency when the pulses of the second and third stages delay relative to the first-stage pulse.

Thus, in the experiment, the photoionisation selectivity  $S = 5.5 \times 10^5$  of the  $^{177\text{m}}\text{Lu}$  isomer has been attained under conditions close to the maximum possible degree of  $^{177\text{m}}\text{Lu}$  extraction, which constitutes 10% when using this channel under conditions when the laser pulses of the second and third stages are delayed relative to the first-stage radiation pulses. The extraction degree can be increased up to 20% by synchronising the pulses and simultaneously reducing the photoionisation selectivity for the 12-13-13-12 channel to  $S = 6 \times 10^3$ .

**Acknowledgements.** The authors express their gratitude to S.S. Arzumanov, Yu.N. Panin, Yu.V. Vyazovetskii, A.V. Kurochkin, and D.Yu. Chuvilin for their help in preparing the  $^{177\text{m}}\text{Lu}$  sample.

The work was supported by the Russian Science Foundation (Project No. 17-13-01180P).

The authors have no conflicts of interest to declare.

## References

1. Banerjee S., Pillai M.R.A., Knapp F.F. *Chem. Rev.*, **115**, 2934 (2015).
2. Dash A., Pillai M.R.A., Knapp F.F. *Nucl. Med. Mol. Imaging (2010)*, **49**, 85 (2015).
3. D'yachkov A.B., Kovalevich S.K., Labozin A.V., Labozin V.P., Mironov S.M., Panchenko V.Ya., Firsov V.A., Tsvetkov G.O., Shatalova G.G. *Quantum Electron.*, **42**, 953 (2012) [*Kvantovaya Elektron.*, **42**, 953 (2012)].
4. D'yachkov A.B., Gorkunov A.A., Labozin A.V., Mironov S.M., Panchenko V.Ya., Firsov V.A., Tsvetkov G.O. *Quantum Electron.*, **48**, 1043 (2018) [*Kvantovaya Elektron.*, **48**, 1043 (2018)].
5. Ageeva I.V., D'yachkov A.B., Gorkunov A.A., Labozin A.V., Mironov S.M., Panchenko V.Ya., Firsov V.A., Tsvetkov G.O., Tsvetkova E.G. *Quantum Electron.*, **49**, 832 (2019) [*Kvantovaya Elektron.*, **49**, 832 (2019)].
6. D'yachkov A.B., Gorkunov A.A., Labozin A.V., Makoveeva K.A., Mironov S.M., Panchenko V.Ya., Firsov V.A., Tsvetkov G.O. *Opt. Spectrosc.*, **128**, 6 (2020) [*Opt. Spektrosk.*, **128**, 10 (2020)].
7. Beekman D.W., Callcott T.A. *Int. J. Mass Spectrom. Ion Phys.*, **34**, 89 (1980).
8. D'yachkov A.B., Gorkunov A.A., Labozin A.V., Mironov S.M., Panchenko V.Ya., Firsov V.A., Tsvetkov G.O. *Prib. Tekh. Eksp.*, **4**, 81 (2018) [*Instrum. Exp. Tech.*, **61** (4), 548 (2018)].
9. D'yachkov A.B., Gorkunov A.A., Labozin A.V., Mironov S.M., Panchenko V.Ya., Firsov V.A., Tsvetkov G.O. *Quantum Electron.*, **48**, 75 (2018) [*Kvantovaya Elektron.*, **48**, 75 (2018)].
10. Bushaw B.A., Nörtershäuser W., Wendt K. *Spectrochim. Acta, Part B*, **54**, 321 (1999).